Bone 64 (2014) 132–137

Contents lists available at ScienceDirect

Bone

journal homepage: www.elsevier.com/locate/bone

Original Full Length Article

Osteocyte apoptosis is required for production of osteoclastogenic signals following bone fatigue in vivo

Oran D. Kennedy [a,1], Damien M. Laudier [a], Robert J. Majeska [a], Hui B. Sun [b,c], Mitchell B. Schaffler [a,*]

[a] Department of Biomedical Engineering, The City College of New York of the City University of New York, New York, NY, USA
[b] Department Radiation Oncology, Albert Einstein College of Medicine, Bronx, NY, USA
[c] Department of Radiation Oncology, Albert Einstein College of Medicine, Bronx, NY, USA

ARTICLE INFO

Article history:
Received 4 November 2013
Revised 7 March 2014
Accepted 27 March 2014
Available online 4 April 2014

Edited by: Mark Johnson

Keywords:
In vivo fatigue
Pan-caspase Inhibitor
Osteocytes
Apoptosis
RANKL
Osteoclasts

ABSTRACT

Osteocyte apoptosis is spatially, temporally and functionally linked to the removal and replacement of microdamage in the bone. Recently we showed that microdamage elicits distinct responses in two populations of osteocytes near the injury site. Osteocytes directly adjacent to microdamage undergo apoptosis, whereas there is a second group of osteocytes located adjacent to the apoptotic population that upregulate expression of osteoclastogenic signaling molecules. In this study we used the pan-caspase inhibitor QVD to test the hypothesis that osteocyte apoptosis is an obligatory step in the production of key osteoclastogenic signals by in situ osteocytes in fatigue-damaged bone. We found, based on real-time PCR and immunohistochemistry assays, that expression of the apoptosis marker caspase-3 as well osteoclastogenic proteins RANKL and VEGF were increased following fatigue, while expression of the RANKL antagonist OPG decreased. However, when apoptosis was inhibited using QVD, these changes in gene expression were completely blocked. This dependence on apoptosis for neighboring non-apoptotic cells to produce signals that promote tissue remodeling also occurs in response to focal ischemic injury in the brain and heart, indicating that osteoclastic bone remodeling follows a common paradigm for localized tissue repair.

Introduction

Osteocyte apoptosis is spatially, temporally and functionally linked to the removal and replacement of fatigue-induced microdamage in bone. Tissue repair is carried out via osteoclastic resorption, which removes damaged tissue, and this is followed by bone formation, which replaces the damaged tissue with new bone. When these processes are coupled together in this way, they are called a Basic Multicellular Unit (BMU) [1]. The mechanisms that initiate and control this process are of considerable interest in terms of fundamental osteocyte and skeletal physiology and for clinical practice, since alterations in BMU-based bone remodeling underlie osteoporosis and several other skeletal pathologies.

Cardoso et al. [2] first demonstrated that osteocyte apoptosis at fatigue microcracks in bone controls the activation and targeting of new resorption foci. Yet the specific contribution of osteocytes to RANKL production has been unclear, despite the longstanding recognition that cells of the osteoblast lineage produce RANKL, which is essential for osteoclast recruitment. Recent studies identified that osteocytes are the dominant source of RANKL in growing mouse bone, and are essential to normal modeling and remodeling at this stage of development [3–5], since osteocyte-specific RANKL knockout (KO) mice have a severe osteopetrotic phenotype. MLO-Y4 osteocyte-like cells also constitutively express RANKL [3,6–8] and thus appear to behave like osteocytes in growing bone.

In contrast, osteocytes in adult bone behave very differently. Kartsogiannis et al. [9] and Kennedy et al. [10] from our laboratory showed that osteocytes in adult bone produce very little RANKL constitutively. However, it was also shown that osteocyte RANKL production is turned on in adult bone by fatigue loading not from the apoptotic osteocytes, but in the neighboring viable osteocytes within a few hundred microns of the damage site and the associated zone of apoptosis. Thus, there are two distinct populations of osteocytes associated with the microdamage sites and their attendant remodeling — dying osteocytes and actively signaling bystanders. What remains unknown is whether these two osteocyte cellular responses to bone microdamage occur in parallel, that is, are independent and simultaneous, or if the osteocyte apoptosis actually triggers RANKL production in neighboring osteocytes. A number of recent studies have suggested the former mechanism [11,12]. In contrast, Cardoso et al. [2] from our laboratory showed that

* Corresponding author at: Department of Biomedical Engineering, The City College of New York, 160 Convent Avenue, Steinman Hall, T-401, New York NY 10031, USA. Fax: +1 212 650 6727.
E-mail addresses: oran.kennedy@nyumc.org (O.D. Kennedy), rmajeska@ccny.cuny.edu (R.J. Majeska), herb.sun@einstein.yu.edu (H.B. Sun), mschaffler@ccny.cuny.edu (M.B. Schaffler).
[1] Current address: Department of Orthopaedic Surgery, New York University School of Medicine, Hospital for Joint Diseases, New York, NY, USA .

http://dx.doi.org/10.1016/j.bone.2014.03.049
8756-3282/

inhibition of osteocyte apoptosis after bone fatigue prevented the onset of bone resorption. However, that study did not establish whether this requirement for osteocyte apoptosis to initiate bone resorption also extends to the triggering of osteoclastogenic cytokine production by non-apoptotic neighboring osteocytes. Therefore, in the current study, we tested these competing hypotheses. Using the same pharmacological approach to modulate osteocyte apoptosis in vivo by means of a pan-caspase inhibitor, we examined osteocyte production of key osteoclastogenic cytokines in response to bone fatigue microdamage.

Materials and methods

In vivo fatigue

Ulnae of female Sprague–Dawley rats were fatigued in end-load bending in vivo to a fixed damage level, in a procedure which has been described in full detail elsewhere [13,14]. Briefly, the right ulnae were fatigued using an electromagnetic loading system (Electroforce 3200, Bose Corp., MN, USA) at peak loads of 16 N at 2 Hz. Bone tissue loses structural stiffness during the formation of fatigue microdamage [15–19], thus changes in ulnar stiffness were monitored from changes in whole bone compliance using the system displacement transducers. Loading was automatically stopped at a stiffness loss of 25%. Furthermore, at the cellular level this loading protocol induces osteocyte apoptosis and subsequent resorption, without resulting in an inflammatory response in the tissue [13,20]. A critical feature of this model is that the baseline remodeling levels in rat ulnar diaphysis is zero. Accordingly, all subsequent remodeling activities can be attributed to our experimental intervention. Loading was carried out under isofluorane anesthesia. Animals had unrestricted cage activity and ad libitum access to food and water before and after loading. Animals were euthanized at 3 and 7 days post loading as previously described and the ulnae dissected free of surrounding soft tissue, and used for either gene expression analyses or immunohistochemical (IHC) studies as described below. It should be noted here that intracortical resorption is normally not present until 10–14 days after loading in this model, thus the 3 and 7 days post loading time-points sampled the activation (pre-resorptive) phase of the response. All procedures were conducted under Institutional Animal Care and Use Committee approval.

Experimental design

Adult rats ($n = 40$) were assigned randomly to one of four experimental groups. Fatigue (FAT) groups were subjected to ulnar fatigue loading and were treated with either vehicle (VEH) or a pan-caspase inhibitor that has been demonstrated to prevent osteocyte apoptosis after bone fatigue in vivo pan-caspase inhibitor, QVD-OPh (quinolyl-valyl-Omethylaspartyl-[-2,6-difluorophenoxy]-methylketone, SM Biochemicals, Anaheim, CA). Beginning 2 h before fatigue loading, one group of animals (FAT + QVD) received the pan-caspase inhibitor at 20 mg/kg/day via (split into two doses, 12 h apart) by IP injection, while a second group (FAT + VEH) received a corresponding dose of the DMSO vehicle (FAT + VEH). The two groups of independent non-fatigued control animals (CON + VEH, CON + QVD) received similar treatments. In this study, independent controls were used rather than the non-loaded contra-lateral limbs, as localized bone injury has been reported in the literature to result in systemic skeletal gene expression responses [21–25].

Gene expression analyses

mRNA levels were measured from mid-diaphyseal segments 6 mm in length (these segments include the sites of microdamage, osteocyte apoptosis and intracortical resorption in this model) to examine the following key osteoclastogenic factors: RANKL, OPG, VEGF and M-CSF. The primer sequences used in these studies are the same as previously reported from our group. We also probed for a range of other pro-inflammatory mediators TNF-α, IL-1, IL-6, IL-11, among others. We previously demonstrated that at the mid-diaphyseal level, the rat ulna has a unique anatomy with a marrow cavity which is very small, comparable in size to cortical bone blood vessels [10]. Thus, following the removal of the periosteum the ulnar diaphyseal tissue segment is highly enriched for osteocytes. Within minutes of death, samples were harvested and flash frozen in liquid nitrogen and were then pulverized using a ball mill (Mikro-Dismembrator, Sartorius, Germany) and total RNA was extracted using the RNeasy-mini kit (Qiagen) with DNase treatment. RNA was quantified, and its quality checked, using a Nanodrop spectrophotometer (Thermo Fisher, Wilmington, DE). Reverse transcription was used to synthesize cDNA by using oligo (dT) primers (Invitrogen, Grand Island, NY). Samples of mRNA (10 ng) were analyzed using real-time PCR with a SYBR green detection system to assess relative gene expression; GAPDH served as the housekeeping gene.

Immunohistochemistry (IHC)

Samples were fixed in buffered formalin, decalcified in formic acid, dehydrated in ethylene glycol monoethyl ether, cleared in methyl salicylate and embedded in an ethyl methacrylate (EMA, Sigma Aldrich) resin. EMA polymerizes at lower temperatures than methyl methacrylate causing less local heating and damage to tissue proteins. We have found that that this also translates to good immunostaining characteristics as well. Bones were embedded in a mixture of 85% EMA–15% n-butyl-phthalate with benzoyl peroxide as a catalyst; processing was carried out at 30 °C. Cross-sections (5 μm thick) were cut from the ulnar mid-diaphyseal region where microdamage, osteocyte apoptosis and bone remodeling occur in this model [4,19,20]. Glass mounted sections were deplasticized, re-hydrated and blocked for endogenous peroxidases by treatment with hydrogen peroxide. Then sections were treated for 30 min with a methanol-NaOH solution for antigen retrieval (DeCal, Biogenex, San Ramon, CA), and blocked for a further 30 min (Rodent Block R, Biocare Medical, Concord, CA). Sections were then incubated overnight in a humidified chamber at 4 °C with antibodies against cleaved caspase-3 (#9661, Cell Signaling Technologies, Danvers MA) RANKL, OPG or VEGF (SC-7628 and SC-8468, Santa Cruz Biotechnology, Santa Cruz, CA). Detection was performed using a goat anti-rabbit secondary antibody with a streptavidin-biotin conjugated system and developed with a DAB substrate chromogen system (Dako, Carpentaria CA), after which the sections were dehydrated and cover-slipped using non-fluorescing mounting medium. Rat tibial growth plates processed in the identical manner were used as positive staining controls, as hypertrophic chondrocytes also express the marker proteins used in these experiments [26–28].

Histomorphometry

Sections were examined and images acquired with a 40× magnification objective under brightfield microscopy. Changes in osteocyte expression of apoptotic and osteoclastic regulatory factors were examined. Thus, the numbers of positively stained osteocytes in microdamage areas (#/mm^2) were then evaluated, where the damage area was defined as two fields of (200 × 200 mm) on either side of the microdamage foci. Measurements were made based on the pattern of osteocyte signaling reported previously by our laboratory [10]. Those studies showed that osteocytes that respond by changing their gene expression profile were localized to within a few hundred microns of microdamage and apoptosis sites.

Statistical analysis

Gene expression and IHC staining data are expressed as mean ± SD. Differences in candidate gene expression levels in fatigue-loaded versus control levels were tested using Student's *t*-test. The Kruskal–Wallis analysis of variance (ANOVA) was used to assess the expression of

factors in osteocytes between groups. Post-hoc comparisons with control values were performed using the Mann–Whitney *U* test.

Results

Gene expression

Neither bone fatigue nor administration of QVD or vehicle altered housekeeping gene (GAPDH) expression at either time-point (Fig. 1 A). Expression of RANKL was increased by >5 and 20 fold ($p < 0.001$) in the FAT + VEH group at 3 and 7 days respectively compared to controls (Fig. 1 B). In contrast the expression of OPG in the FAT + VEH group was significantly reduced at both time-points (Fig. 1 C).

In the FAT + QVD treated group, in which the same level of damage was induced but osteocyte apoptosis was inhibited, there was no change in either RANKL or OPG expression. QVD treatment had no effect on baseline RANKL or OPG expression in control groups, ruling out the possibility of a direct action of QVD on osteocyte RANKL or OPG expression. Thus, the lack of change in RANKL or OPG in the FAT + QVD group must be the result of apoptosis suppression. VEGF expression was negligible in control tissues, but was increased in the FAT + VEH group at 7-days post fatigue; VEGF levels in the FAT + QVD group were unchanged from baseline (Fig. 1 D). M-CSF expression was low in controls and remained unchanged by bone fatigue.

Immunohistochemistry

As in numerous previous studies, bone fatigue (FAT + VEH) caused a dramatic and highly significant increase in the numbers of Cas-3 positive stained osteocytes at both 3 and 7 days after loading (8 and 5-fold increases, respectively over CON + VEH; $p < 0.001$ Fig. 2 A). These increases in osteocyte apoptosis were completely prevented by QVD treatment. IHC results for osteocyte RANKL, OPG and VEGF expression mirrored the gene expression results described above. At 3 days, osteocyte RANKL and VEGF staining at microdamage foci were markedly increased in FAT + VEH bone (6 and 4-fold respectively compared to FAT + QVD and control groups, $p < 0.001$, Fig. 2 B, D) while the constitutive OPG staining was decreased by approximately 20% ($p < 0.01$, Fig. 2 C), a similar trend persisted at 7 day time-points (Fig. 3).

Inhibition of osteocyte apoptosis (FAT + QVD) completely prevented the increases in the number of RANKL- and VEGF-expressing osteocytes. QVD treatment did not alter the number of OPG expressing osteocytes in control bones (CON + QVD), confirming the lack of direct pharmacological effect for QVD on osteoclastogenic cytokine expression observed in the gene expression studies.

Discussion

Bone remodeling of fatigue-induced microdamage is an essential tissue repair mechanism, which is known to require osteocyte apoptosis as an initiating step [2]. However, dying cells do not themselves produce essential osteoclastogenic cytokines, including RANKL [10]. Rather, the cells responsible for this task comprise a population of neighboring osteocytes that surround the damaged area and its apoptotic osteocytes yet remain viable. The current studies demonstrate that the rapid and robust expression of osteoclastogenic cytokines by these viable osteocytes, which ensues following fatigue loading-induced microdamage in vivo, is also completely dependent on osteocyte apoptosis. The response, at both the RNA and protein levels, was completely abrogated when damage-induced osteocyte apoptosis was inhibited pharmacologically using a pan-caspase inhibitor. Thus, these results establish that microdamage alone is not a sufficient stimulus to trigger RANKL signaling from osteocytes. Instead, the stimulus that induces viable osteocytes to produce the cytokines required to initiate osteoclast recruitment and differentiation arises as a direct consequence of the apoptosis of their neighbors.

While production of RANKL for osteoclast recruitment has long been acknowledged as a property of osteoblast-lineage cells, the recognition that osteocytes play a central role in RANKL production is much more recent. However, the demonstration of this novel role for osteocytes has been largely limited to growing bone, where most osteocytes express RANKL [3,29]. Interestingly this phenotype is reflected in

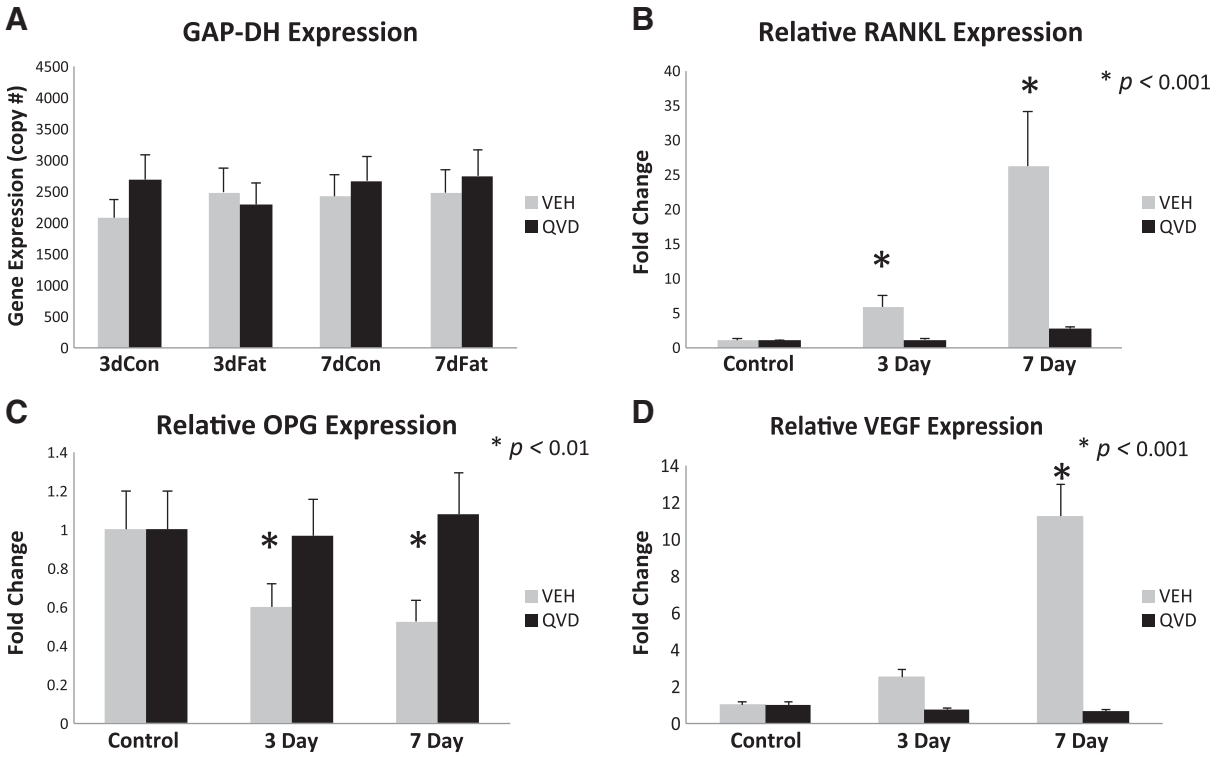

Fig. 1. (A) Copy number of GAPDH in all four experimental groups. Relative gene expression of (B) RANKL (C) OPG and (D) VEGF.

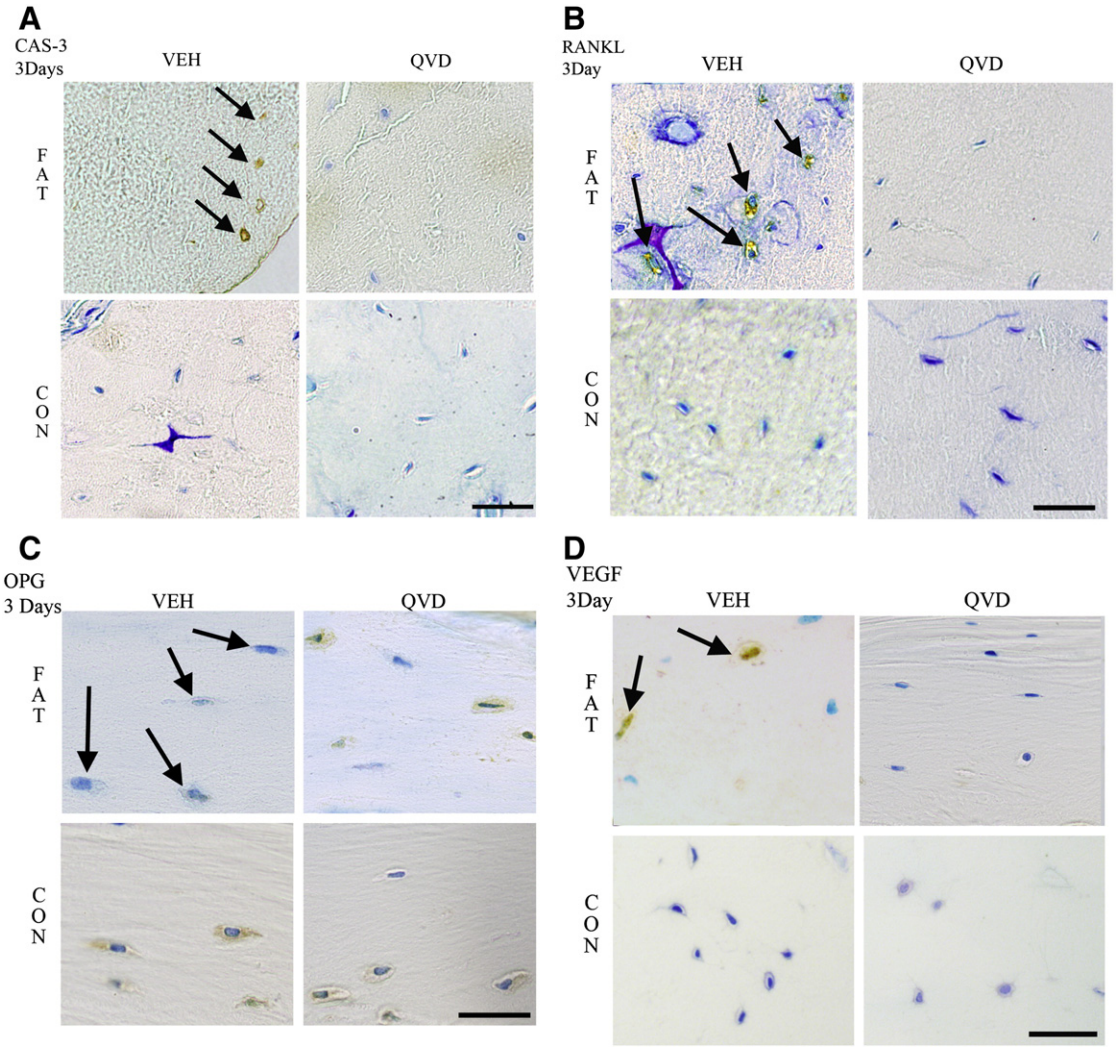

Fig. 2. Immunohistochemistry images taken at 40× magnification of decalcified ulnar cross sections stained for (A) Caspase 3 and pro-osteoclastogenic factors RANKL, OPG and VEG-F (B, C and D, respectively), counterstained with toluidine blue at 3-days post-fatigue. Scale bar = 50 μm.

constitutive expression of RANKL by MLO-Y4 osteocyte-like cells [3–5]. Furthermore, the profound osteopetrosis and deficiencies in modeling and remodeling in osteocyte-specific RANKL knockout mice are consequences of RANKL deficiencies during development [3,5]. Evidence from Kartsogiannis et al. [9], Kennedy et al. [10] and the current studies indicate that osteocytes in adult bone behave differently, in that they express very little RANKL constitutively. Yet osteocyte production of RANKL in adult bone is turned on at microdamage sites, and the trigger for that RANKL production is localized osteocyte apoptosis. The finding that RANKL expression by viable osteocytes is completely dependent on apoptosis of nearby osteocytes further suggests that this relationship applies in other circumstances where a causal relationship between osteocyte apoptosis and the initiation of bone resorption has been established [30].

In previous studies from our laboratory, it was shown that RANKL production was turned on in the localized population of viable osteocytes adjacent to those undergoing apoptosis. This suggests the existence of a "penumbra effect", whereby surviving osteocytes surround or 'wall-in' the damaged matrix and its associated apoptotic osteocytes. These osteoclastogenic signals in osteocytes were absent in animals subjected to identical microdamage levels, but which were treated with QVD, a pan-caspase inhibitor of apoptosis. The idea that there might be discrete groups of both dying and locally responding viable osteocytes at bone microdamage sites was first suggested by Verborgt et al. [14], who noted that apoptotic osteocytes at microdamage were surrounded by a localized "ring" of osteocytes that protected themselves against apoptosis by upregulating production of the anti-apoptotic protein Bcl-2. Moreover, the extent and position of the RANKL (and VEGF) expressing osteocytes our recent studies, and the Bcl-2 expressing osteocytes in the Verborgt are similar and suggest that these actively responding osteocyte groups population may be the same. Recent reports in the literature have shown that Bcl-2 is also critically involved in the autophagy pathway. A recent study by Onal et al examined the effect of knocking out Atg-7, a gene that is essential for autophagy, from osteocytes [31]. This resulted in decreased trabecular bone volume and cortical thickness and increased intracortical porosity — thus effectively mimicking the impact of aging on bone tissue. Furthermore, Jilka et al. [32] recently found that when apoptosis was genetically abrogated in osteoblasts and osteocytes via the selective deletion of Bak and Bax genes, the osteocytes that could not undergo apoptosis became stressed and dysfunctional. These dysfunctional cells also increased production of RANKL and VEGF, which resulted in extensive intracortical resorption in the mouse long bones.

The current studies of bone fatigue microdamage show that signals emanating from apoptotic osteocytes trigger osteoclastogenic cytokine production in neighboring viable osteocytes. The nature of these signals is currently unknown. Although we did screen for inflammatory mediators that could be involved (TNF-α, IL-1, IL-6, IL-11 and others), these data unfortunately yielded no insights into this issue. The fundamental mechanism of tissue repair whereby apoptotic cells trigger neighboring

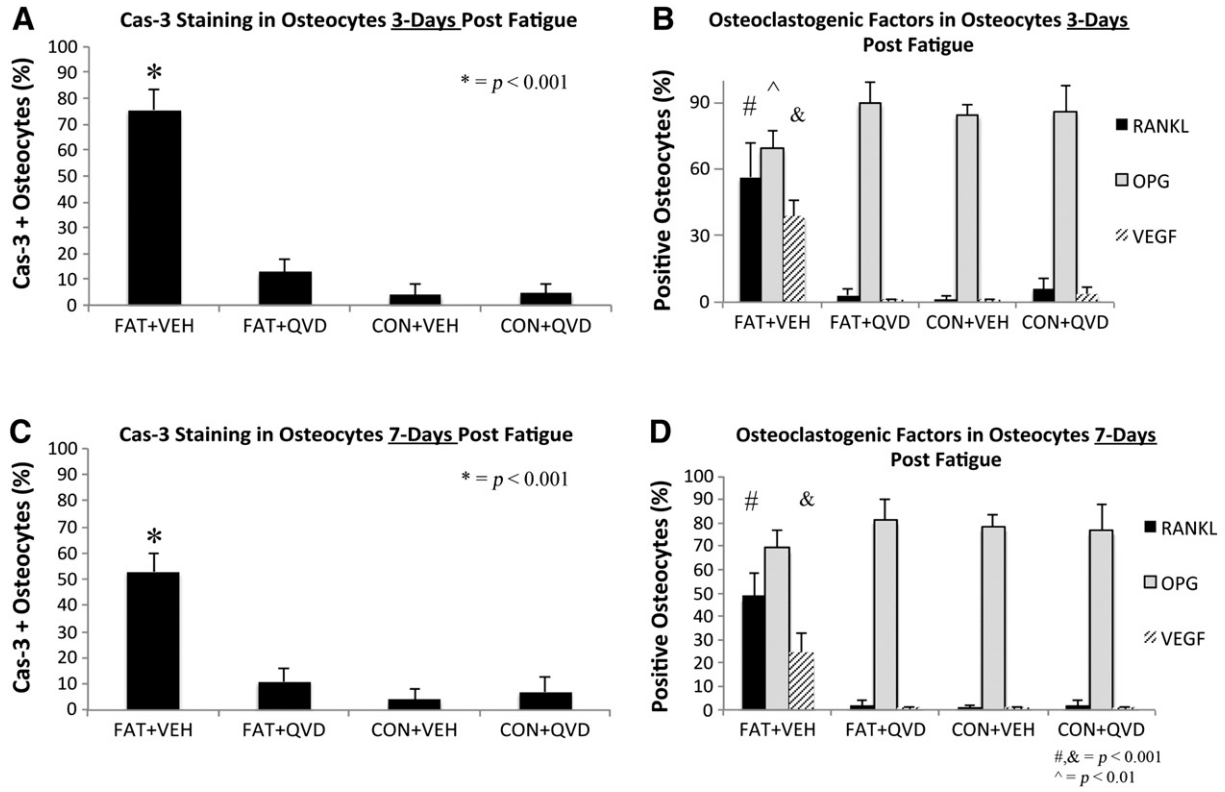

Fig. 3. Graph showing percentage of osteocytes staining for (A) Caspase 3 at 3-days (B) RANKL, OPG and VEGF at 3-days (C) Caspase 3 at 7-days and (D) RANKL, OPG and VEGF at 7-days.

cells to produce key regulatory cytokines has been described in other systems, for example in focal brain and heart ischemia, retinal, corneal and skin injury healing. There, the initial lesion (which is analogous to a microcrack in our fatigue model) results in a central core of cell death. This region is removed by phagocytic cells and replaced with new cells and tissue. Within hours after the onset of cell death, apoptotic cells in the core region release acute signals that trigger the viable cells in a penumbra region surrounding the area of focal injury to produce pro-inflammatory factors and cytokines (e.g., TNFα, HIF1α, VEGF, MCPs, others) that attract monocytes and macrophages to the injury site [33,34]. Precise timing of these events and the particular combination of regulatory cytokines appear to be unique to each tissue (brain, myocardium, bone, etc.), but the general pattern is consistent among highly diverse systems. In other focal injuries, this coordinate activation and responses of cells in the penumbra regions surrounding a "core" of apoptotic cell has been referred to as a "*Bystander phenomenon*", the process whereby cells in close proximity to dying cells are either protected or sensitized as a consequence of their location [33,35-40]. Our studies suggest that the pattern of cellular and signaling events in remodeling of microdamage in bone seems analogous to those seen in other focal micro-injuries. We showed that intact non-apoptotic osteocytes immediately surrounding apoptotic ones at microcracks in bone turn on production of RANKL and VEGF, which are obligate regulators of bone remodeling, and the triggering of their production is dependent upon the local cell death.

The nature of the signaling from dying osteocytes that might trigger changes in osteoclastogenic cytokine expression from neighboring bystander osteocytes in situ is not known. Indeed, the broader issue of how apoptotic cells signal to their neighbor is a fundamental question at the forefront of apoptosis research in general. Speculations about potential signals from apoptotic osteocyte have focused on events that occur and molecules that are released late in the cell death process after membrane breakdown. Others have suggested that apoptotic bodies could be a potential signal from dying to neighboring osteocytes [41,42]. However, movement of apoptotic bodies in canaliculi is unlikely due to physical limitations. Apoptotic bodies are ~20–1000 nm in diameter, while the sieving properties of the pericellular matrix surrounding osteocyte processes only permit movement of solutes of less than 70 kDa (≈6 nm diameter) [42,43]. Thus, apoptotic debris cannot serve as significant signal among osteocytes in situ. A number of in vitro studies have shown that necrotic and apoptotic cells release several large intracellular proteins like HMGB1 as well as double-stranded DNA fragments [44–46]. Bidwell et al showed that apoptotic MLOY4 cells release HMGB1, which stimulated TNFα and RANKL synthesis in bone marrow stromal cells [47]. However, HMGB1 stimulation of RANKL in healthy osteocytes independent of TNFα is not shown. Critically, recent data show that factors like HMGB1 and double-stranded DNA fragments are released late in apoptosis, after cell membrane integrity is lost [45], while in vivo the activation of RANKL by apoptotic osteocyte occurs quickly before cell degradation is seen. Alternatively, a number of studies over the last decade have established that cells in the early stage of apoptosis release 'find me' signals that stimulate activation and migration of professional phagocytes which remove dying cells [48–51]. Several soluble chemoattractant 'find-me' signals released during the early phase of apoptosis have been defined, including triphosphate nucleotides (ATP/UTP), lysophosphatidylcholine and the chemokine CX3CL1. These small molecules diffuse readily through the local tissue to bind to appropriate receptors on the responding cells. The potential roles for such 'find me' signals in osteocyte apoptosis triggering of RANKL expression is currently unknown and requires future investigation.

In summary, these data establish that the causal relationship between osteocyte apoptosis near microdamage includes an early osteoclastogenic signaling response by adjacent viable osteocytes. This also offers further support to the idea that osteocytes in this system respond to microinjury through a penumbra effect i.e. the osteoclastogenic signaling cells surrounding those that are undergoing apoptosis, which is known to occur at sites of microscopic damage in other tissues.

Conflict of interest

All authors have no conflict of interest.

Acknowledgments

This work was supported by NIH grants AR41210, AR057139 and AR060445 (MBS) and AR050968 (HBS).

References

[1] Burr DB, Martin RB, Schaffler MB, Radin EL. Bone remodeling in response to in vivo fatigue microdamage. J Biomech 1985;18(3):189–200.
[2] Cardoso L, Herman BC, Verborgt O, Laudier D, Majeska RJ, Schaffler MB. Osteocyte apoptosis controls activation of intracortical resorption in response to bone fatigue. J Bone Miner Res 2009;24(4):597–605.
[3] Nakashima T, Hayashi M, Fukunaga T, Kurata K, Oh-Hora M, Feng JQ, et al. Evidence for osteocyte regulation of bone homeostasis through RANKL expression. Nat Med 2011;17(10):1231–4.
[4] O'Brien CA, Nakashima T, Takayanagi H. Osteocyte control of osteoclastogenesis. Bone 2012;4(2):258–63.
[5] Xiong J, O'Brien CA. Osteocyte RANKL: new insights into the control of bone remodeling. J Bone Miner Res 2012;27(3):499–505.
[6] You L, Temiyasathit S, Lee P, Kim CH, Tummala P, Yao W, et al. Osteocytes as mechanosensors in the inhibition of bone resorption due to mechanical loading. Bone 2008;42(1):172–9.
[7] Zhao S, Zhang YK, Harris S, Ahuja SS, Bonewald LF. MLO-Y4 osteocyte-like cells support osteoclast formation and activation. J Bone Miner Res 2002;17(11):2068–79.
[8] Al-Dujaili SA, Lau E, Al-Dujaili H, Tsang K, Guenther A, You L. Apoptotic osteocytes regulate osteoclast precursor recruitment and differentiation in vitro. J Cell Biochem 2011;12(9):2412–23.
[9] Kartsogiannis V, Zhou H, Horwood NJ, Thomas RJ, Hards DK, Quinn JM, et al. Localization of RANKL (receptor activator of NF kappa B ligand) mRNA and protein in skeletal and extraskeletal tissues. Bone 1999;25(5):525–34.
[10] Kennedy OD, Herman BC, Laudier DM, Majeska RJ, Sun HB, Schaffler MB. Activation of resorption in fatigue-loaded bone involves both apoptosis and active pro-osteoclastogenic signaling by distinct osteocyte populations. Bone 2012;50(5):1115–22.
[11] Mulcahy LE, Taylor D, Lee TC, Duffy GP. RANKL and OPG activity is regulated by injury size in networks of osteocyte-like cells. Bone 2011;48(2):182–8.
[12] Hazenberg JG, Freeley M, Foran E, Lee TC, Taylor D. Microdamage: a cell transducing mechanism based on ruptured osteocyte processes. J Biomech 2006;39(11):2096–103.
[13] Bentolila V, Boyce TM, Fyhrie DP, Drumb R, Skerry TM, Schaffler MB. Intracortical remodeling in adult rat long bones after fatigue loading. Bone 1998;23(3):275–81.
[14] Verborgt O, Gibson GJ, Schaffler MB. Loss of osteocyte integrity in association with microdamage and bone remodeling after fatigue in vivo. J Bone Miner Res 2000;15(1):60–7.
[15] Carter DR, Hayes WC. Compact bone fatigue damage II: a microscopic examination. Clin Orthop 1977;127:265–74.
[16] Caler WE, Carter DR, Harris WH. Techniques for implementing an in vivo bone strain gage system. J Biomech 1981;14(7):503–7.
[17] Schaffler MB, Burr DB. Stiffness of compact bone: effects of porosity and density. J Biomech 1988;21(1):13–6.
[18] Vashishth D. Rising crack-growth-resistance behavior in cortical bone: implications for toughness measurements. J Biomech 2004;37(6):943–6.
[19] Vashishth D, Koontz J, Qiu SJ, Lundin-Cannon D, Yeni YN, Schaffler MB, et al. In vivo diffuse damage in human vertebral trabecular bone. Bone 2000;26:147–52.
[20] Silva MJ, Touhey DC. Bone formation after damaging in vivo fatigue loading results in recovery of whole-bone monotonic strength and increased fatigue life. J Orthop Res 2007;25(2):252–61.
[21] Schaffler MB, Li XJ, Jee WS, Ho SW, Stern PJ. Skeletal tissue responses to thermal injury: an experimental study. Bone 1988;9(6):397–406.
[22] Einhorn TA, Simon G, Devlin VJ, Warman J, Sidhu SP, Vigorita VJ. The osteogenic response to distant skeletal injury. J Bone Joint Surg Am 1990;72(9):1374–8.
[23] Li XJ, Jee WSS. Adaptation of diaphyseal structure to aging and decreased mechanical loading in the adult rat - a densitometric and histomorphometric study. Anat Rec 1991;229(3):291–7.
[24] Suva LJ, Seedor JG, Endo N, Quartuccio HA, Thompson DD, Bab I, et al. Pattern of gene expression following rat tibial marrow ablation. J Bone Miner Res 1993;8(3):379–88.
[25] Yamazaki M, Majeska RJ, Yoshioka H, Moriya H, Einhorn TA. Spatial and temporal expression of fibril-forming minor collagen genes (types V and XI) during fracture healing. J Orthop Res 1997;15(5):757–64.
[26] Ballock RT, O'Keefe RJ. The biology of the growth plate. J Bone Joint Surg Am 2003;85-A(4):715–26.
[27] Ohashi N, Robling AG, Burr DB, Turner CH. The effects of dynamic axial loading on the rat growth plate. J Bone Miner Res 2002;17(2):284–92.
[28] Silvestrini G, Ballanti P, Patacchioli F, Leopizzi M, Gualtieri N, Monnazzi P, et al. Detection of osteoprotegerin (OPG) and its ligand (RANKL) mRNA and protein in femur and tibia of the rat. J Mol Histol 2005;36(1–2):59–67.
[29] Xiong J, Onal M, Jilka RL, Weinstein RS, Manolagas SC, O'Brien CA. Matrix-embedded cells control osteoclast formation. Nat Med 2011;17(10):1235–41.
[30] Emerton KB, Hu B, Woo AA, Sinofsky A, Hernandez C, Majeska RJ, et al. Osteocyte apoptosis and control of bone resorption following ovariectomy in mice. Bone 2010;46(3):577–83.
[31] Onal M, Piemontese M, Xiong J, Wang Y, Han L, Ye S, et al. Suppression of autophagy in osteocytes mimics skeletal aging. J Biol Chem 2013;288(24):17432–40.
[32] Jilka RL, O'Brien CA, Roberson PK, Bonewald LF, Weinstein RS, Manolagas SC. Dysapoptosis of osteoblasts and osteocytes increases cancellous bone formation but exaggerates bone porosity with age. J Bone Miner Res 2014;29(1):103–17.
[33] Fisher M. The ischemic penumbra: identification, evolution and treatment concepts. Cerebrovasc Dis 2004;17(Suppl. 1):1–6.
[34] Katsman D, Zheng J, Spinelli K, Carmichael ST. Tissue microenvironments within functional cortical subdivisions adjacent to focal stroke. J Cereb Blood Flow Metab 2003;23(9):997–1009.
[35] Cusato K, Bosco A, Rozental R, Guimaraes CA, Reese BE, Linden R, et al. Gap junctions mediate bystander cell death in developing retina. J Neurosci 2003;23(16):6413–22.
[36] Cusato K, Zakevicius J, Ripps H. An experimental approach to the study of gap-junction-mediated cell death. Biol Bull 2003;205(2):197–9.
[37] Elshami AA, Saavedra A, Zhang H, Kucharczuk JC, Spray DC, Fishman GI, et al. Gap junctions play a role in the 'bystander effect' of the herpes simplex virus thymidine kinase/ganciclovir system in vitro. Gene Ther 1996;3(1):85–92.
[38] Spray DC, Hanstein R, Lopez-Quintero SV, Stout Jr RF, Suadicani SO, Thi MM. Gap junctions and Bystander Effects: Good Samaritans and executioners. Wiley Interdiscip Rev Membr Transp Signal 2013;2(1):1–15.
[39] Udawatte C, Ripps H. The spread of apoptosis through gap-junctional channels in BHK cells transfected with Cx32. Apoptosis 2005;10(5):1019–29.
[40] Perez Velazquez JL, Kokarovtseva L, Sarbaziha R, Jeyapalan Z, Leshchenko Y. Role of gap junctional coupling in astrocytic networks in the determination of global ischaemia-induced oxidative stress and hippocampal damage. Eur J Neurosci 2006;23(1):1–10.
[41] Kogianni G, Mann V, Ebetino F, Nuttall M, Nijweide P, Simpson H, et al. Fas/CD95 is associated with glucocorticoid-induced osteocyte apoptosis. Life Sci 2004;75(24):2879–95.
[42] Li W, You L, Schaffler MB, Wang L. The dependency of solute diffusion on molecular weight and shape in intact bone. Bone 2009;45(5):1017–23.
[43] Wang L, Wang Y, Han Y, Henderson SC, Majeska RJ, Weinbaum S, et al. In situ measurement of solute transport in the bone lacunar-canalicular system. Proc Natl Acad Sci U S A 2005;102(33):11911–6.
[44] Munoz LE, Peter C, Herrmann M, Wesselborg S, Lauber K. Scent of dying cells: the role of attraction signals in the clearance of apoptotic cells and its immunological consequences. Autoimmun Rev 2010;9(6):425–30.
[45] Silva MT. Secondary necrosis: the natural outcome of the complete apoptotic program. FEBS Lett 2010;584(22):4491–9.
[46] Silva MT, do Vale A, dos Santos NM. Secondary necrosis in multicellular animals: an outcome of apoptosis with pathogenic implications. Apoptosis 2008;13(4):463–82.
[47] Bidwell JP, Yang J, Robling AG. Is HMGB1 an osteocyte alarmin? J Cell Biochem 2008;103(6):1671–80.
[48] Elliott MR, Chekeni FB, Trampont PC, Lazarowski ER, Kadl A, Walk SF, et al. Nucleotides released by apoptotic cells act as a find-me signal to promote phagocytic clearance. Nature 2009;461(7261):282–6.
[49] Elliott MR, Ravichandran KS. Clearance of apoptotic cells: implications in health and disease. J Cell Biol 2010;189(7):1059–70.
[50] Ravichandran KS. Find-me and eat-me signals in apoptotic cell clearance: progress and conundrums. J Exp Med 2010;207(9):1807–17.
[51] Ravichandran KS. Beginnings of a good apoptotic meal: the find-me and eat-me signaling pathways. Immunity 2011;35(4):445–55.